Coastal Dynamics 2017
Paper No. 249

PROJECION OF FUTURE CHANGE IN STORM SURGE USING MRI-AGCM3.2H ENSEMBLE EXPERIMENTS

Yosuke Yamamoto[1], Tomohiro Yasuda[2], Nobuhito Mori[3] and Hajime Mase[4 1]

Abstract

Recent researches have shown that the intensity of tropical cyclones (TCs) will be stronger due to climate change, and the extreme of storm surge inundation in coastal area may increase. In such conditions, the projection of the change in storm surge under global warming is important to prepare appropriate coastal disaster adaptation strategy. Many projects to utilize ensemble experiments for climate change projection are ongoing in order to quantify and minimize the uncertainty. This study conducts storm surge simulations targeting Japan using the outputs of ensemble climate experiments by general circulation model (GCM) to project the future change in storm surge and discusses the effect of simulation conditions of the climate models such as spatial distributions of sea surface temperature, cumulus parameterization schemes, and initial values of atmosphere. The results indicate that increase of storm surge height due to climate change depends on the location and is expected to increase by 0.15 to 0.45 m.

Key words: storm surge, future projection, ensemble experiment, cumulus scheme, sea surface temperature

1. Introduction

Many studies have been performed on the changes of tropical cyclones (TCs) due to climate change. According to the Fifth Assessment Report (AR5), published by the Intergovernmental Panel on Climate Change (IPCC), it is reports that "*Warming of the climate system is unequivocal.*", and that "*It is likely that the global frequency of occurrence of cyclones will either decrease or remain essentially unchanged, concurrent with a likely increase in both global mean tropical cyclone maximum wind speed and precipitation rates*". Increasing risk of the storm surge disaster due to the TC characteristic change makes it important to project and estimate the future change in storm surges under global warming scenarios for the mitigation around the coastal areas and cities.

Methods for projecting the future change of storm surge can be classified into a dynamic method and a statistical method. The statistical method is useful for climate study because of its low computational cost, although it has model dependent bias or error in comparison with dynamic modeling. This study employs the dynamic method for storm surge projections in order to quantify and evaluate the several return periods' surge height around Japan. Disadvantage of using the dynamic method is the limitation of data obtained from atmospheric projections, the uncertainty due to the small number of storm surge simulations and the spatial resolution.

The projection of storm surge is highly depend on the forcing (i.e. GCM projections). More precise climate experiments and future predictions are available with the development of finer resolution climate models in comparison with IPCC Fourth Assessment Report (2007) and the downscaling studies; these outputs are able to be used for the storm surge simulations. However, future climate experiments using higher resolution models have been performed only for small number of cases due to their high computational costs. Thus, the future storm surge predictions using these data still remain uncertainty.

[1]Graduate School of Engineering, Kyoto University, Japan. yamamoto.yosuke.34m@st.kyoto-u.ac.jp
[2]Faculty of Environmental and Urban Engineering, Kansai University, Japan. tomo@oceanwave.jp
[3]Disaster Prevention Research Institute, Kyoto University, Japan. mori@oceanwave.jp
[4]Disaster Prevention Research Institute, Kyoto University, Japan. mase.hajime.5c@kyoto-u.ac.jp

Now it is a benefit that ensemble experiments using the 60-km high-resolution atmospheric general circulation model, developed by the Meteorological Research Institute (Kitoh et al., 2011; MRI-AGCM3.2H, GCM60 hereafter), can be used to increase the number of storm surge simulations even if the reproduction of the weather disturbance and TCs is not accurate enough due to the 60-km resolution with the bias compared to finer atmospheric data. For this model bias in the 60-km data, a correction method has been proposed by Yasuda et al. (2015). This method regards the outputs from a 5-km resolution regional climate model (RCM5 hereafter) as the true values of sea level pressure (SLP) and wind speed (U10) data at the level of 10 m height from the surface. After applying the bias correction of 60-km coarse data by 5-km fine data, storm surge calculations are conducted by using the corrected data directly as input external forcing data, and the future a return period's values of storm surge are demonstrated. This bias correction method is very useful when using GCM output for the storm surge calculations as accurate as using RCM5 output.

This study estimates future change in storm surge considering uncertainty using GCM60 ensemble experiment outputs of multi-SSTs (sea surface temperatures) and multi-schemes of cumulus parameteriza-tion. The purpose of this study is to quantify and minimize the uncertainty by applying the above mentioned bias correction method for these ensemble members in order to increase the number of TCs and samples for the analysis. In addition, the influence of the simulation conditions (cumulus parameterization schemes, SSTs, and initial conditions) on the future storm surge height is discussed.

2. Ensemble climate change experiments

Many ensemble climate experiments have been performed in order to quantify the reliability and certainty of predictions under the global warming scenarios. The Innovation Program of Climate Change Projection for the 21th Century (KAKUSHIN Program, 2007-2011) used MRI-AGCM3.2H and conducted ensemble climate change experiments for the present climate and future one (Murakami et al., 2012). Furthermore, the Program for Risk Information on Climate Change (SOUSEI Program, 2012-2016) used the similar model as MRI-AGCM3.2H and conducted ensemble experiments not only for multi-SSTs but also for different initial conditions (Ogata et al., 2017).

The KAKUSHIN program used the observed SST by the UK Met Office Hadley Centre (HadlSST) for the present and four different projections of SSTs for the future as boundary conditions in GCM experiments. The SOUSEI program, the different initial value of atmosphere (i2) is used for the GCM projections based on the KAKUSHIN program run (hereinafter referred to as i1). Both programs used three cumulus parameterization schemes for clouds: Kain-Fritsch (KF), Yoshimura (YS), and Arakawa-Schubert (AS), respectively. Mizuta et al. (2012) reported that the simulation result using the YS scheme is more realistic than that using the AS scheme. Furthermore, this study confirmed that the TC genesis number using the AS scheme is extremely small compared to the observation and the other models. For these reasons, this study does not use the output using the AS scheme, and only use the results using the YS scheme and the KF scheme for the further analysis. Table 1 shows the case codes for the ensemble experiments used in this study. This study employs 4 present and 16 future ensemble experiment results for storm surge simulations. Also the present climate experiment using the RCM5 is denoted as RCM5P. The calculation for both present and future climate have been performed for 25 years, and its period for the present climate is 1979-2003, and for the future climate is 2075-2099.

Table 1. Ensemble experiments and case codes

Initial condition			Kakushin (i1)		Sousei (i2)	
Cumulus scheme			Yoshimura	Kain-Fritsch	Yoshimura	Kain-Fritsch
SST	Present (1979-2003)		YS_P_i1	KF_P_i1	YS_P_i2	KF_P_i2
	Future (2075-2099)	cluster0	YS_Fc0_i1	KF_Fc0_i1	YS_Fc0_i2	KF_Fc0_i2
		cluster1	YS_Fc1_i1	KF_Fc1_i1	YS_Fc1_i2	KF_Fc1_i2
		cluster2	YS_Fc2_i1	KF_Fc2_i1	YS_Fc2_i2	KF_Fc2_i2
		cluster3	YS_Fc3_i1	KF_Fc3_i1	YS_Fc3_i2	KF_Fc3_i2

This study extracted the TCs from the each of the ensemble simulations using the TC track data, using the TC detection method developed by Murakami et al (2010). The target TCs in this study are the TCs which pass the area shown as D2 in Figure1, which includes the regions from Kyushu to Kanto, and for each TC, a storm surge calculation is conducted using the SLP and the U10, after performing the bias correction. In this study, we define the TC approaching period as the period when the center of the TC is in the D1, and the TC influenced area as the 50 grids from the center to the north, south, east and west (D1: 1 grid = 12150 m), 1215 km in total. The ratio of the grid size between each domain is 3:1. (D2: 1 grid = 4050 m, D3/ D4 =1050 m)

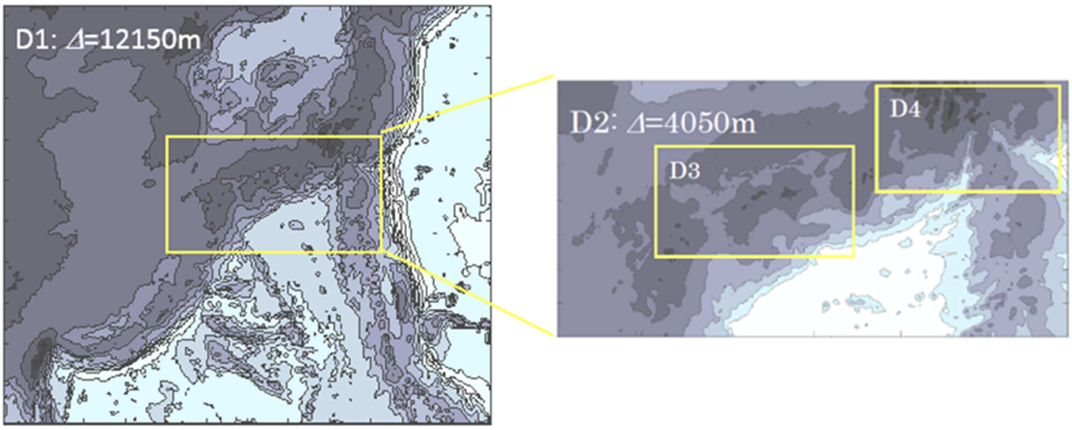

Figure 1. Domain area used in storm surge calculation

3. Bias correction method

The bias correction method for SLP and U10 that treats the outputs from RCM5 as true values, developed by Yasuda et al. (2015), is employed for all the 4 present ensembles and 16 future ensembles. This method consists of the following three steps: 1) interpolation of the temporal resolution (6 hours to 30 minutes), 2) approximation of the probability density function of SLP and U10, and 3) considering the land effect for reduction of U10. The details of these correction methods are shown below.

3.1. *Interpolation of the temporal change*

A spatial-temporal interpolation is performed for the SLP and U10 data of the TC among the output using GCM60 ensembles. The data output interval of GCM60 is 6 hours, whereas the data interval of RCM5 is 30 minutes. The results of the storm surge calculations using 6 hourly SLP and U10 data as input external forcing data cannot reproduce surges correctly due to coarse time interval for storm surge modeling. Therefore, the GCM60 data is linearly spatially interpolated to assume continuous liner TC movement on 30 minutes' intervals. The procedure of this correction method is as follows: the determination of the trajectory of TC, the determination of the change of SLP and U10 data, and then estimates the movement of TC. Figure 2 shows the example of the correction performance. This method produces a more continuous TC behavior, and it is expected to improve the estimations of storm surges in the calculation.

3.2. *Adjustment of the probability density function of SLP and U10*

This method corrects the model bias of GCM60 by regarding the output of RCM5 as the true value, and applies bias correction (that is, adjustment) for the occurrence probability distribution for SLP and U10 data of GCM60 output to approximate the occurrence frequency to that of RCM5. In Yasuda et al. (2015), six different methods are analyzed and determined that the use of the normal type distribution is the lowest

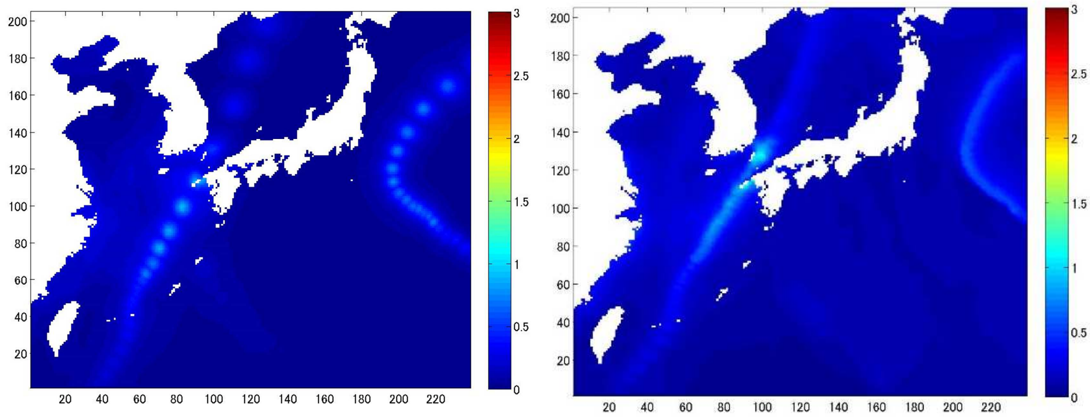

Figure 2. Example of the interpolation of temporal resolution

computational cost and the highest correction accuracy. In the normal distribution type bias correction, normal distribution is applied to the parametric type correction used by Piani et al. (2010). This method consists of three steps. First, extract minimum pressure and maximum wind speed in the TC approaching period from both RCM5 and GCM60 ensembles. Second, assume that these distributions follow the normal distribution. Third, approximate the probability distribution by correcting the average value and the standard deviation of GCM60 data to that of RCM5. The correction formula used is as shown below.

$$x'_{GCM} = \frac{\sigma_{RCM}}{\sigma_{GCM}}(x_{GCM} - \mu_{GCM}) - \mu_{RCM} \tag{1}$$

where x'_{GCM} is the GCM60 output after correction, σ_{RCM} is the standard deviation of RCM5 output, σ_{GCM} is the standard deviation of GCM60 output, x_{GCM} is the GCM60 output, μ_{RCM} is the average value of RCM5, and μ_{GCM} is the average value of GCM60. The region for correction is the TC influenced area defined above.

Figure 3 shows an example of this bias correction applied to both SLP (left) and U10 (right). The red broken line shows the cumulative probability of GCM60 data before the correction, the red solid line shows that of GCM60 after correction, and the blue line shows that of RCM5. These figures indicate that although large discrepancy was seen before the correction, it is getting very small after the correction. On the other hand, the correction accuracy in places where the wind speed or the central pressure is strong is still low meaning there is still room for improvement on the correction function.

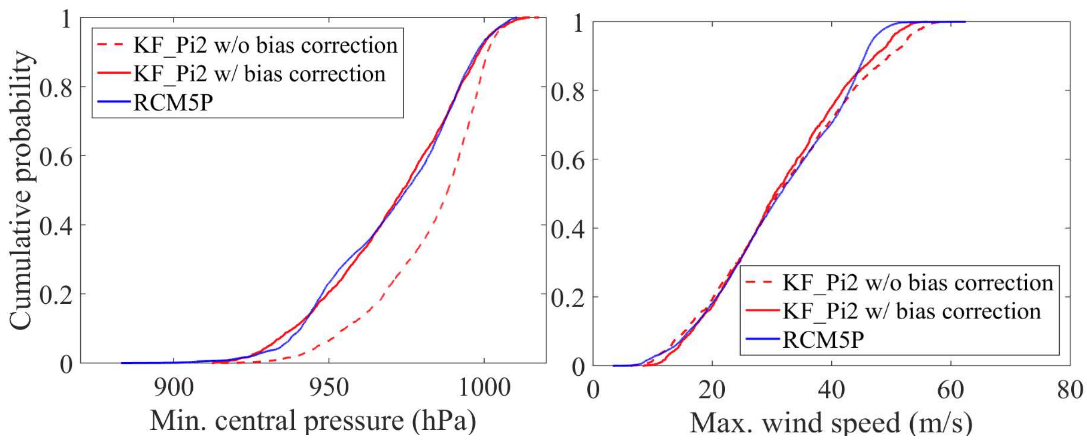

Figure 3. Cumulative probability distribution of SLP(left) and U10 (right) of KF_P_i2
before/after the correction for GCM60 output (red: dotted, solid line), RCM5P output (blue solid line)

The same correction is used for the output of future climate projections. This study assumes that the biases in the future climate is the model bias caused by using the different cumulus convention schemes, and used the same correction value used in the present climate for the future climate.

3.3. *Bias correction of the probability density function wind on land*

Recent study showed that the simulated surge heights using 60 km grid atmospheric data tend to higher than those using finer grid data (e.g. 20 km GCM). One of the factors of being higher surge height is whether or not the climate model considers the influence on land wind. That is, wind speeds near the coasts using coarse grid become stronger due the less land effects of coarse grid information. Therefore, the bias of wind on land and near coast should be corrected by using the normal distribution type bias correction method for outputs of GCM60. This method consists of two steps; First, the U10 data on land in D2 is extracted from each of the GCM60 ensembles and the RCM5P by using the land data. This study used the land data of the later mentioned storm surge model SuWAT. Second, the distribution of GCM60 outputs is approximated to that of RCM5 outputs.

Figure 4 shows an example of applying this correction method on the wind on land. Before the correction is not done, the wind is not weaken on land, meaning that GCM60 does not consider the effect of land. However, wind is weaken during passing the land after the correction. The bias correction enabled to consider the land effect even with the output using GCM60.

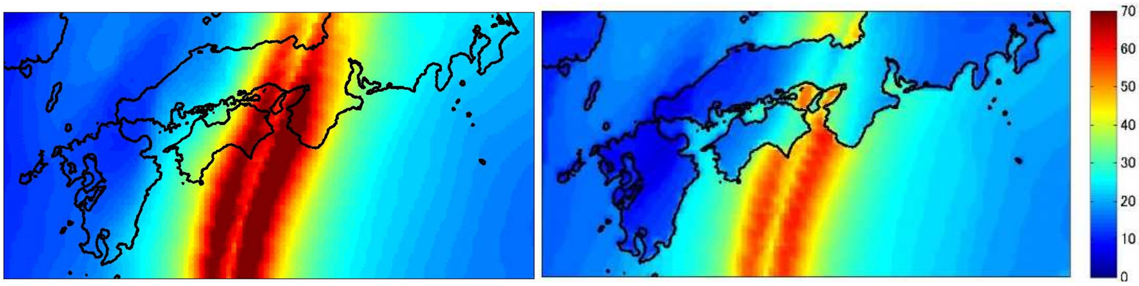

(a) Before the correction (b) After the correction

Figure 4. Example of applying the correction method for the wind on land

4. Methods of storm surge simulation

After applying the bias correction to GCM60 output, a series of storm surge simulations was conducted using the Surge, Wave and Tide model (SuWAT) developed by Kim et al. (2008). The governing equations of the surge module are the non-linear shallow water equation as follows:

$$\frac{\partial \eta}{\partial t}+\frac{\partial M}{\partial x}+\frac{\partial N}{\partial y}=0 \qquad (2)$$

$$\frac{\partial M}{\partial t}+\frac{\partial}{\partial x}\left(\frac{M^2}{d}\right)+\frac{\partial}{\partial y}\left(\frac{MN}{d}\right)=$$

$$-gd\frac{\partial \eta}{\partial x}-\frac{1}{\rho_w}d\frac{\partial P}{\partial x}+\frac{1}{\rho_w}(\tau_s^x-\tau_b^x+F_x)+A_h\left(\frac{\partial^2 M}{\partial^2 x}+\frac{\partial^2 M}{\partial^2 y}\right)+fN \qquad (3)$$

$$\frac{\partial N}{\partial t}+\frac{\partial}{\partial x}\left(\frac{MN}{d}\right)+\frac{\partial}{\partial y}\left(\frac{N^2}{d}\right)=$$

$$-gd\frac{\partial \eta}{\partial y}-\frac{1}{\rho_w}d\frac{\partial P}{\partial y}+\frac{1}{\rho_w}(\tau_s^y-\tau_b^y+F_y)+A_h\left(\frac{\partial^2 N}{\partial^2 x}+\frac{\partial^2 N}{\partial^2 y}\right)+fM \tag{4}$$

where, η is water level from free surface, M and N are flow flux in x and y directions, d is water depth, g is the acceleration due to gravity, f is the Coriolis parameter, ρ_w is fluid density of sea water, P is pressure, τ_s is surface shear stress, τ_b is bottom shear stress, F_x and F_y are radiation stresses, and A_h is viscosity coefficient.

Storm surge simulation is performed using the SLP and U10 data after the bias correction, obtained from each of the ensembles, directly as the driving force for SuWAT. SuWAT employs a parallel nesting scheme. Simulation results of domain D2 with grid size 4050 m as shown in Figure 1 are used as boundary conditions for domain D3 and D4 every time steps. In the following analysis output of D3 and D4 are overlaid on the results of D2. Then, the extreme value statistical analysis is performed using the maximum storm surge heights against the obtained maximum values at each grid. This study used the Gumbel distribution as the extreme value distribution function, and the Gringorten formula as the plotting position formula. The return period of extreme value statistics is set to 25 years to match the period of the climate change experiments.

5. Results and discussion

5.1. *Verification for the present climate*

To investigate the effect of the initial conditions on the spatial storm surge distributions, the results of the ensembles calculated on the different initial conditions but using the same cumulus scheme are used for the analysis. Although no big difference was seen in most of the area, ±1.0 m surge height difference was seen in specific bay-scale area. Yasuda et al. (2015) noted that the obtained storm surge in these areas tend to depend on the presence or absence of the several strong TCs. Therefore, this study investigated the relationship between the storm surge and the track of strong TCs over 940 hPa. Then, it was found that the presence or absence of a strong TC coincides with the high or low storm surge and different initial condition generates the different strength and the track of TCs in the specific area and ends up making a difference in long-term storm surge height.

This study assumed the result of each ensemble simulation is independent from each other and each result of 25 years result from each cumulus scheme is put together to be regarded as 50 years calculations in total. Thus, 50 years return period storm surge heights are analyzed using another storm surge distribution.

Figure 5 shows the spatial storm surge distributions for each cumulus scheme. Hereafter the storm surge distribution made from 50 years calculation using KF scheme is referred to as KF_P50, and that of using YS scheme is referred to as YS_P50. These are considered to be more reliable distributions by increasing the number of samples and reducing the uncertainty of TC track.

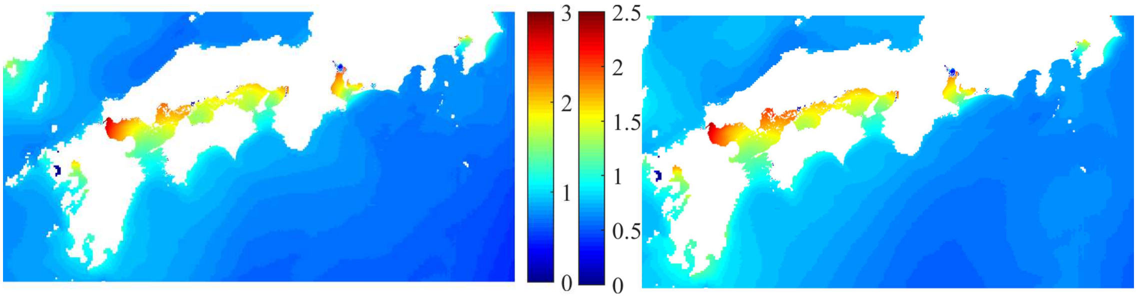

Figure 5. Storm surge distributions for KF_P50 and YS_P50

The effect of the cumulus scheme used in GCM60 simulation on the storm surge is investigated. Figure 6 shows the difference of the storm surge distributions obtained from the respective cumulus schemes in the present climate (KF_50 and YS_P50). This figure shows negative values in almost the whole area. Results indicate that the KF scheme tends to predict smaller storm surge values than the YS scheme, indicating that the different schemes simulate different tendencies of TCs. Due to the apparent differences in using the different schemes, this study considers the future change separately for these models.

Figure 6. The difference of the storm surge distributions using different cumulative schemes (KF scheme - YS scheme)

5.2. *Verification for the future climate*

5.2.1. Future change projection of storm surge

The storm surge calculations were done for the 16 future climate experiments in the same way as above. This study considered the change of long-term storm surge by extreme value statistical analysis, by using the simulated values of maximum storm surge. The future changes of maximum storm surge under the different conditions are calculated by subtracting present results from future results for all the 16 ensemble members. This study uses the KF_P50 and YS_P50 as the storm surge distribution in the present climate.

Figure7 shows the mean and variance of future change of the ensembles around Japan. As for the average shown in Figure 7(a), storm surge is smaller in the southern part of Kyushu region and Ise Bay by about 0.10 m, and is higher in the Ariake Sea, Seto Island Sea, and the eastern part of Wakayama by 0.30 m. Overall, the storm surge tends to be same or lower in western Japan, and tends to be higher in eastern Japan, suggesting that the higher region of the storm surge will shift toward east. Mori et al. (2012) denoted that the appearance and disappearance positions of TCs are shifting eastward in the case of the northwest Pacific Ocean, and is shifting northward in latitude direction. Results of this study matches to the result by Mori et al. (2012) on the TCs future change tendency, and can be regarded as the tendency of storm surge distribution shifts to the east along with the change of the TC route. However, the variance shown in Figure 7 (b) indicates that the variance is high in specific areas, e.g. Ariake Sea and Seto Island Sea, which means the remaining of the uncertainties in the future predictions.

In order to analyze the scatter in these areas, this study selects six areas (Ariake Sea, Suou Nada Sea area, Aki Nada Sea area, Osaka Bay, Ise Bay, and Tokyo Bay) shown in Figure 8(a) and conducts further investigation on the change of the storm surge. Figure 8(b) shows the box plot of maximum value of 16 different future changes for each area. From this figure, the maximum change of storm surge in these six areas increases by 0.15 to 0.45 m on average and its value is increasing from western Japan to eastern Japan. On the other hand the scatter in these areas is still large and its value varies more than 1 m between the minimum and the maximum change, so further investigation is required.

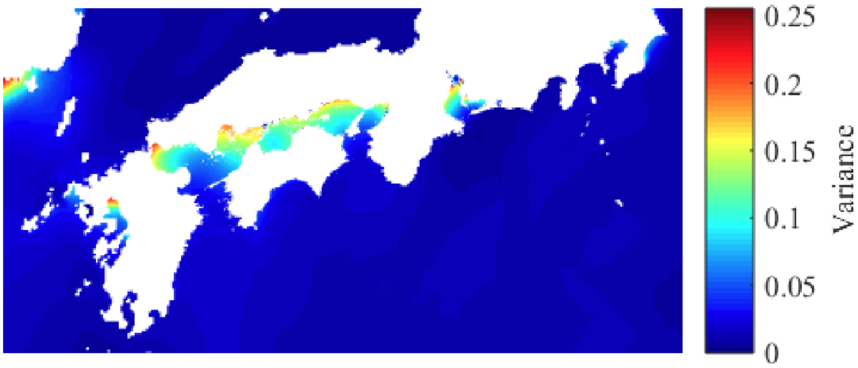

(a) Average

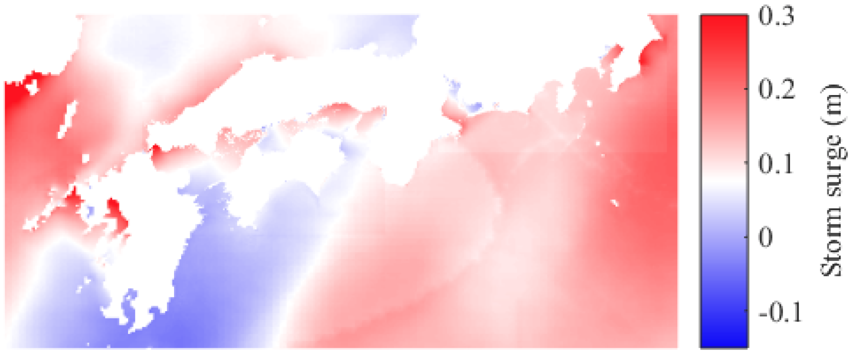

(b) Variance

Figure 7. The mean value of the 16 future changes

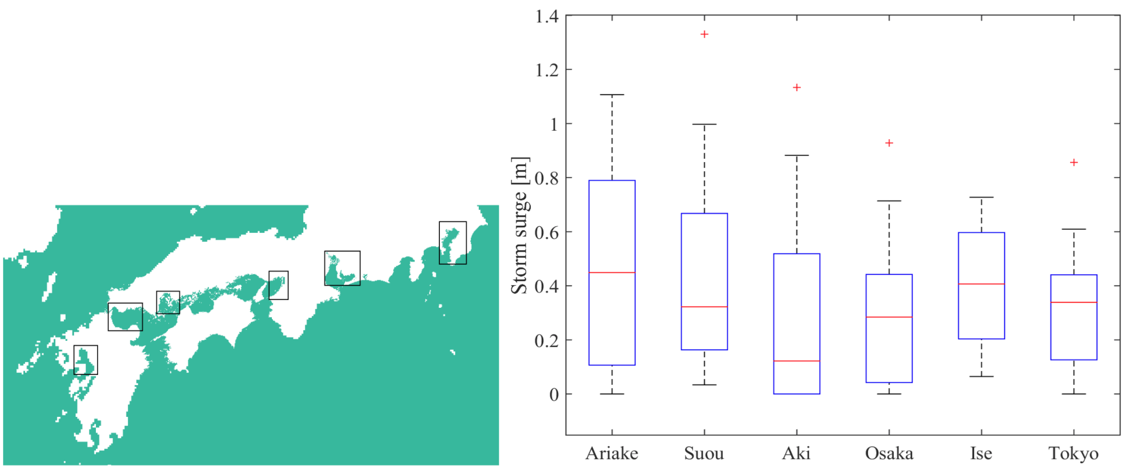

Figure 8. (a) Selected six areas for analysis (Ariake Sea, Suou Nada Sea area, Aki Nada Sea area, Osaka Bay, Ise Bay, and Tokyo Bay), (b) The box plot of the maximum changes for each area (red: average, black: maximum and minimum change, blue: first and third quantile line, red +: outlier)

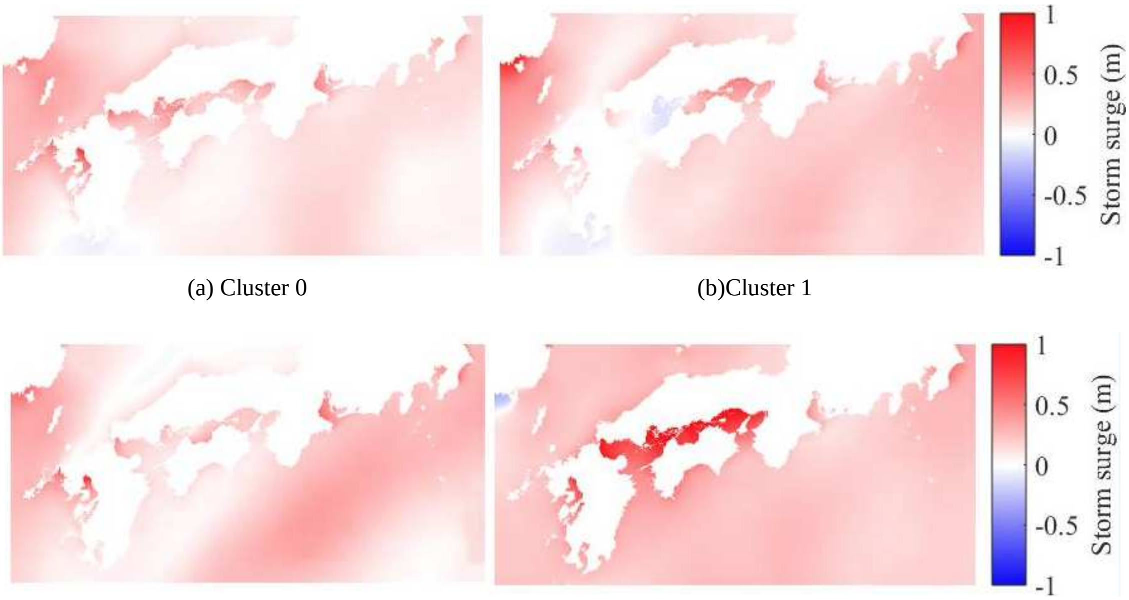

(a) Cluster 0 (b)Cluster 1

(c) Cluster2 (d) Cluster 3

Figure 9. The future change of storm surge for each SST in KF_F_i2

5.2.2. SST dependence on future change of storm surge

This research considers the effect of the SSTs on the storm surge by comparing the results obtained under the four different SSTs. In KAKUSHIN program, the four SSTs for the future climate were analyzed from 18 models of CMIP3 under the SRES A1B scenario and grouped into three SST pattern clusters (cluster 1-3) and also got ensemble mean of all models (cluster0). In SOUSEI program, SSTs as boundary condition for the future experiment is analyzed from 28 models of CMIP5 and classified into four SSTs in the same way.

Figure 9 shows the future change of storm surge for four different SST ensembles, calculated using the KF scheme under the initial value of i2. In the classification of future SST change tendency by Murakami et al. (2012), the temperature rise tendency close to Japan show similar tendency in cluster 0 and cluster 2, smaller tendency in cluster 1, and large tendency in cluster 3. In Figure 9, the spatial storm surge distribution in cluster 0 and cluster 2 is similar, smaller change in cluster 0, and larger in cluster 3, indicating that the storm surge is dependent on SSTs.

6. Conclusions

This study developed and applied a bias correction method to the outputs of 60 km GCM ensemble experiment outputs using multiple SSTs spatial distributions, multi cumulus parameterization schemes, and multi atmospheric initial conditions under the global warming scenarios (SRES A1B and RCP8.5). Then, a series of storm surge simulation was performed using the SLP and U10 data after the bias correction for GCM60 as the direct external forcing. The future change projection of storm surge around Japan was performed, and the effect of the simulation conditions on the storm surge distribution is evaluated. By taking the average of 16 ensemble storm surge distributions, the distribution discussing the uncertainty of initial conditions, cumulus parameterization schemes, and SSTs is made.

Proposed bias correction method works well and be able to improve accuracy and reliability of the outputs of GCM60. The effect of the cumulus scheme used in GCM60 simulation on the storm surge is investigated and indicated the different schemes simulate different tendencies of TCs. The overall tendency of the storm surge distribution around Japan is a shift towards east which agrees with previous study on future change in TCs. The maximum changes of storm surge in any of the bays increased by 0.15 to 0.45m. However, the dispersion in bay scale is high, and needs more detailed analysis. The spatial distribution of storm surge is affected by the difference of SST ensembles.

Acknowledgements
This study was conducted under the Program for Risk Information on Climate Change (SOUSEI) and Grant-in-Aid of the Ministry of Education, Culture, Sports, Science and Technology (MEXT).

References

IPCC AR4: Climate Change 2007: The Physical Science Basis. Contribution of Working Group I to the Fourth Assessment Report of the Intergovernmental Panel on Climate Change, Cambridge University Press, 996p., 2007.

IPCC AR5: Climate Change 2013: The Physical Science Basis. Working Group I Contribution to the Fifth Assessment Report of the Intergovernmental Panel on Climate Change, Cambridge University Press, 1535p., 2013

Kain, J. S. and J. M. Fritsch: A one-dimensional entraining/detraining plume model and its application in convective parameterization. J. Atmos. Sci., Vol.47, pp.2784–2802, 1990.

Kim, S.Y., T. Takayama, T. Yasuda, H. Mase: Effects of large Tidal Variation on Storm Surges and Waves, Annual Journal of Coastal Engineering, JSCE, Vol.54, pp.276–280, 2007.

Kitoh, A., S. Kusunoki, T. Nakaegawa: Climate Change Projection over South America in the late 21st century with the 20 and 60 km mesh Meteorological Research Institute Atmospheric General Circulation Model (MRI-AGCM), Journal of Geographical Research, Vol 116, Issue D6, 2011.

Mizuta, R., H. Yoshimura, H. Murakami, M. Matsueda, H. Endo, T. Ose, K. Kamiguchi, M. Hosaka, M. Sugi, S. Yukimoto, S. Kusunoki, and A. Kitoh: Climate Simulations Using MRI-AGCM3.2 with 20-km Grid, J. Meteor. Soc. Japan, Vol.90A, pp.232–258, 2012.

Mori, N., H. Murakami, T. Shimura, S. Nakajo, T. Yasuda, H. Mase: Multi-Model Ensemble Projection of Future Tropical Cyclone Characteristics due to Global Climate Change, Journal of Japan Society of Civil Engineers, Ser. B2 (Coastal Engineering), Vol.68, No.2, pp.1251–1255, 2012.

Murakami, H. and M. Sugi: Effect of Model Resolution on Tropical Cyclone Projections, SOLA, Vol.6, pp.73–76, 2010.

Murakami, H., R. Mizuta, E. Shindo: Future changes in tropical cyclone activity projected by multi-physics and multi-SST ensemble experiments using the 60-km-mesh MRI-AGCM, Climate Dynamics, Volume 39, Issue 9, pp.2569–2584, 2012.

Ogata, T., R. Mizuta, K. Yoshida. "Effect of high-resolution SST on East Asian summer monsoon and tropical cyclone activity in a 60-km AGCM." Hydrological Research Letters, 10.3, 95–100, 2016.

Piani, C., J.O. Haerter, E. Coppola: Statistical bias correction for daily precipitation in regional climate models over Europe, Theoretical and Applied Climatology, 99, pp.187–192, 2010.

Randall, D. A. and D. M. Pan: Implementation of the Arakawa-Schubert cumulus parameterization with a prognostic closure. Meteorological Monographs. Vol.24, No.46, pp.137–147, 1993.

Research and Development Bureau, Ministry of Education, Culture, Sports. Science and Technology, Japan: Utilization of climate model data for impact assessment, pp.4–11, 2014.

Yasuda, T., S. Nakajo, S.Y. Kim, Mori N., Mase H., Horsburgh K.: Evaluation of Storm Surge Risk Directly Based on Climate Change Projetion, Journal of Japan Society of Civil Engineers, Ser. B2 (Coastal Engineering), Vol.67, No.2, pp.I_1171–I_1175, 2011.

Yasuda, T., N. Katahira, N. Mori, H. Mase, Y. Shibutani: Projection for future change of storm surges around Japanese Coasts using Non-hydrostatic RCM outputs, Journal of Japan Society of Civil Engineers, Ser. B2 (Coastal Engineering), Vol.69, No.2, pp.I_1261–I_1265, 2013.

Yasuda, T., N. Katahira, N. Mori, H. Mase, Y. Shibutani: Development of statistical bias correction method for climate model typhoons and ensemble future storm surge projection due to climate change, Journal of Japan Society of Civil Engineers, Ser. B2 (Coastal Engineering), Vol.71, No.2, pp.I_1507–I_1512, 2015.

Yoshimura, H., R. Mizuta, H. Murakami: A Spectral Cumulus Parameterization Scheme Interpolating Between Two Convective Updrafts with Semi-Lagrangian Calculation of Transport by Compensatory Subsidence. Mon. Wea. Rev., Vol.143, No.2, pp.597–621, 2015.